BRILL
WAGENINGEN
ACADEMIC

JOURNAL OF INSECTS AS FOOD AND FEED (2026) DOI:10.1163/23524588-BJA10443

Journal of Insects as Food and Feed
brill.com/jiff

RESEARCH ARTICLE

Modulation of lipidomic and proteomic profile by diet composition in black soldier fly

*Guido Domingo[1], Matteo Miceli[2], Daniele Bruno[3], Marco Orlando[2,#], Donatella Caruso[4,5], Fiorenza Farè[5], Manuela Fontana[5], Lorenzo Bonesini[2], Gianluca Tettamanti[3,7], Gianluca Molla[2], Morena Casartelli[6,7] and Loredano Pollegioni[2]**

[1]Plant Physiology Laboratory, Department of Biotechnology and Life Sciences, University of Insubria, via J.H. Dunant 3, 21100 Varese, Italy; [2]The Protein Factory 2.0 laboratory, Department of Biotechnology and Life Sciences, University of Insubria, via J.H, Dunant 3, 21100 Varese, Italy; [3]Insect Science and Biotechnology laboratory, Department of Biotechnology and Life Sciences, University of Insubria, via J.H. Dunant 3, 21100 Varese, Italy; [4]Laboratory of Biochemistry and Molecular Biology of Metabolism – Mass Spectrometry "Giovanni Galli", Department of Pharmacological and Biomolecular Sciences "Rodolfo Paoletti", University of Milano, via Balzaretti 9, 20133 Milan, Italy; [5]Unitech OMICs, Mass Spectrometry Facility, University of Milano, Viale Ortles 22, 20139 Milan, Italy; [6]Insect Physiology and Biotechnology laboratory, Department of Biosciences, University of Milano, via G. Celoria 26, 20133 Milan, Italy; [7]Interuniversity Center for Studies on Bioinspired Agro-environmental Technology (BAT Center), University of Napoli Federico II, Piazza Carlo di Borbone 1, 80055 Portici, Italy;
*loredano.pollegioni@uninsubria.it

[#]Present address: Laboratory of Environmental and Life Sciences, University of Nova Gorica, Vipavska cesta 13, Rožna Dolina, 5000 Nova Gorica, Slovenia

Received 19 November 2025 | Accepted 22 June 2026 | Published online 13 July 2026

Abstract

Within the framework of a circular bioeconomy, the valorisation of organic waste streams into high-value biomolecules represents a sustainable strategy to reduce environmental burdens while generating renewable resources. In this context, the black soldier fly (*Hermetia illucens*, BSF) has emerged as an effective biocatalyst for converting the organic fraction of municipal solid waste (OFMSW) into high-value biomolecules. We investigated how two surrogate OFMSW substrates (s-OFMSW and a nutrient-modified variant) and two developmental stages (last-instar larvae and 4-day-old pupae) shape BSF biomass composition. Lipidomic and proteomic profiles were characterised and analysed by two-way ANOVA, clustering, pathway enrichment, and cross-omics correlation. Protein isolates showed high purity with stage- and diet-dependent solubility; essential amino acids were comparatively enriched in larvae. The developmental stage was the main driver of lipidomic variation, whereas diet more strongly influenced the proteome, particularly in pupae. Larvae reared on the lipid-rich s-OFMSW accumulated energy-dense lipids (such as triacylglycerols and fatty acids), consistent with metabolic demands preceding metamorphosis. Pupae showed increased fatty acid esters of hydroxy fatty acids and diacylglycerols and uniquely accumulated monoacylglycerols, phosphatidylserines/ethanolamines and acylcarnitines, reflecting lipid mobilisation and membrane remodelling. The modified s-OFMSW promoted the accumulation of structural lipids (sphingomyelins, lysophosphatidylcholines) together with triacylglycerol storage. Lipid pathway enrichment consistently highlighted glycerophospholipid metabolism, and integrative analyses revealed coordinated regulation

across proteins and metabolites. Overall, diet composition and developmental stage jointly and predictably modulate BSF lipid and protein landscapes and chitin yields, enabling rational optimisation of rearing strategies to tailor biomass quality for feed, materials, and other biotechnological applications.

Keywords

extraction methods – fatty acids – green chemistry – *Hermetia illucens* – proteins

1 Introduction

In recent years, the black soldier fly (BSF, *Hermetia illucens*) has emerged as a promising biotechnological tool for the conversion of organic waste and by-products into high value biomolecules that, in turn, can be used as row materials for several applications, a process in line with circular bioeconomy principles (Bruno *et al.*, 2025b; Tettamanti and Bruno, 2024). A sustainable, straightforward workflow, that uses an integrated fractionation procedure combining defatting, alkaline protein solubilisation and acid selective precipitation, for the extraction and separation of proteins, lipids, and chitin from BSF larvae has been proposed by (Caligiani *et al.*, 2018). Moreover, specific procedures for the extraction of lipids and proteins have been reported (Leni *et al.*, 2017; Caligiani *et al.*, 2018; Bonomini *et al.*, 2024). The residual organic fraction represents the source for the extraction of chitin. Recently, we improved the extraction of biomolecules from BSF (Bruno *et al.*, 2025a–c), demonstrating that larvae reared on the organic fraction of municipal solid waste (OFMSW) yield high-purity biomolecule fractions. That study specifically focused on protein recovery, and the fraction we obtained had a significant degree of purity, suitable for developing conductive biodegradable protein-based plastic films (Testa *et al.*, 2025a). Unfortunately, the overall extraction process was energy-intensive especially because of the defatting step (Bruno *et al.*, 2025b). However, very recently, for the isolation of the chitin fraction, a novel green and sustainable pipeline employing deep eutectic solvents (DES) (i.e., menthol:lactic acid and choline chloride:lactic acid) combined with microwave-assisted extraction has been developed (Miceli *et al.*, 2024). This methodology allows bypassing the energy-demanding defatting step leading to the recovery of high-quality chitin while allowing >80% solvent reuse. This method represents one of the few approaches for chitin preparation from insects that, being based on DES, is truly green and aligns with sustainability criteria that avoids hazardous reagents while enabling efficient recovery of chitin from insect biomass (Mersmann *et al.*, 2025).

Focusing on the industrial application of the three main components (proteins, lipids, and chitin), lipid fractions, primarily composed of medium-chain saturated and monounsaturated fatty acids such as lauric and oleic acid, are well-suited for both feed and non-food applications, including biodiesel production (Mohan *et al.*, 2023). Beyond feed, the valorisation of lipids and free fatty acids extracted from insects also includes their use as surfactants (Franco *et al.*, 2021). Protein isolates from BSF larvae are being increasingly studied for their nutritional potential in aquaculture, poultry, and pet feed, as they offer a balanced amino acid profile rich in lysine, leucine, aspartic and glutamic acid (Macwan *et al.*, 2024). Moreover, the emulsifying and gelling capabilities of BSF protein extracts make them suitable for novel food formulations (Kumar *et al.*, 2022). In cosmetic and pharmaceutical formulations, hydrolysed BSF proteins and lipids (based on the high lauric acid content, approx. 40-60%) show promising bioactive properties, including antioxidants, antimicrobial, and anticancer activities (Franco *et al.*, 2022; Praseatsook *et al.*, 2025). Lastly, high-purity BSF proteins have been used to produce functional materials such as biodegradable bioplastics possessing interesting properties such as high conductivity and flexibility (Bruno *et al.*, 2025b; Testa *et al.*, 2025a,b). Concerning chitin and its deacetylated derivative, chitosan, which are obtained from the exoskeleton, these biomolecules possess significant potential as functional polymers (Witono *et al.*, 2024). Their antimicrobial, film-forming, and metal-chelating properties have led to applications in wastewater treatment, wound healing, controlled drug delivery, and biodegradable packaging (Chicea *et al.*, 2024; Siddiqui *et al.*, 2024). Notably, BSF-derived chitin has been also used in developing hydrogels, nanocomposites, and scaffolds for tissue engineering, showing comparable or superior performance to crustacean-derived materials, as well as to produce high-quality chitosan with tailored physicochemical characteristics (Giani *et al.*, 2025).

Despite growing interest in BSF-derived products, significant knowledge gaps remain regarding the standardised characterisation and functional properties of its protein, lipid, and chitin fractions, as well as their safety and variability across production and processing systems, which currently limit their optimised and large-scale exploitation not only in food and feed applications (Bruno *et al.*, 2026), but also for advanced applications in biomedical, biotechnological, and agricultural sectors (Tettamanti and Bruno, 2024). Moreover, the valorisation strategies collectively underscore the economic and environmental viability of BSF-based biorefineries and reinforce their role as pivotal elements in the transition to bio-based circular value chains. For these reasons, the present study aims to investigate how the composition of the rearing substrate and its nutrient content affect the qualitative and quantitative profiles of lipids and proteins extracted from BSF larvae and pupae. In particular, the larvae were reared on two substrates formulated to mimic the OFMSW. The use of these artificial diets, whose composition reflects the variability of this waste (Fisgativa *et al.*, 2016), ensures that the experiments are conducted under reproducible and standardised conditions. Understanding the relationship between the chemical composition of the OFMSW and the macromolecule profile obtained from the insect biomass at the end of the bioconversion process is essential for developing a supply chain supporting OFMSW treatment and valorisation.

2 Materials and methods

Insect rearing

BSF rearing was performed as reported in (Pimentel *et al.*, 2017). Briefly, after oviposition, newly hatched larvae were reared on two experimental substrates mimicking the OFMSW: "s-OFMSW", which contained higher amounts of proteins, lipids and polysaccharides on both an "as fed" and "dry matter" basis, and "modified s-OFMSW", in which simple sugars were more abundant (see Tables S1 and S2 in the Supplementary materials for the composition of both substrates). In both cases, "s" stands for "surrogate", as previously reported by Bruno *et al.* (2025a). Moreover, the composition of a real OFMSW (r-OFMSW) was used as a reference, for the sake of comparison (Table S2 in the Supplementary materials). Before feeding the larvae, all ingredients used for the preparation of s-OFMSW and modified s-OFMSW were thoroughly mixed and homogenised using a shredder to obtain the final substrates. Batches of 300 larvae were grown in plastic containers (16 × 16 × 9 cm), fed with the selected diets, and maintained in the dark at 27 ± 0.5 °C and 70 ± 5% relative humidity for the whole larval period. Once insects reached the appropriate developmental stage for the analyses (i.e., last instar larvae and 4-day-old pupae) (Bruno *et al.*, 2025b), they were collected from the substrate, washed to remove food debris, frozen at –20 °C for 24 hours and then dried at 60 °C overnight. Subsequently, the different samples were processed as reported below.

Protein and lipid extraction

The extraction procedure was carried out from five biological replicates for each condition (last instar larvae and 4-day-old pupae grown on both substrates), and each analysis was repeated at least three times. For each replicate, the procedure was carried out using 20 g of frozen biomass, desiccated in an oven at 60 °C overnight. Each dried-frozen sample was ground with an IKA A10 laboratory grinder for 2 min and 20 000 rpm, and used for extraction (Bruno *et al.*, 2025b).

Briefly, lipids were extracted by Soxhlet extraction (Caligiani *et al.*, 2018) with petroleum ether for 18 h. Extracted lipids were stored at –20 °C and unfrozen only prior to the analysis.

Proteins were extracted from the lipid-free solid following a modified procedure from (Smets *et al.*, 2020) based on dispersion in demineralised water adjusted at pH 11 with a 1.0 M NaOH solution (the condition of maximum solubility), centrifugation and filtration. While the supernatant was adjusted to pH 4.0 with a 1.0 M HCl solution (the condition of minimum solubility) to precipitate the proteins, the solid fraction containing chitin was stored at –80 °C (Bruno *et al.*, 2025b).

Total carbohydrate, ash and chitin content

The non-chitin polysaccharides along with the total sugar content were determined on 100 mg of ground sample added with 10 ml of 3 M HCl and boiled for 3 hours; the solution was neutralised with Na_2CO_3 at room temperature. 1 ml of the solution was centrifuged at 16 000×*g* for 15 min at room temperature. The reducing carbohydrate content was measured with the phenol-sulfuric acid method (Sadasivam and Manickam, 2005; Bruno *et al.*, 2025b). The potential contribution of chitin to the carbohydrate content was determined by preparing a standard curve with 1 mg/ml N-acetyl-D-glucosamine (Merck, St. Louis, MO, USA).

The chitin was extracted according to the formic acid/sodium hydroxide method by (Hahn *et al.*, 2022) using 3 g of the defatted, deproteinised samples (Bruno

et al., 2025b). The extraction yield was calculated as the weight ratio (%) of the dried and bleached chitin extract to the initial dried insect sample.

Ashes were determined according to UNI EN 14775 by sample incineration at 550 °C for 8 hours. They were calculated as the weight ratio (%) of the ashes to the initial dried insect sample.

Composition of protein extracts

The total protein concentration was determined by acid hydrolysis followed by the ninhydrin assay (Starcher, 2001). The protein yields were calculated as the weight ratio (%) of the dried protein extract to the initial dried insect sample weight. Furthermore, the composition of the protein extracts was determined to assess its purity (expressed as protein content percentage) by determining the residual carbohydrate contents, as reported below. Protein secondary structure composition was determined by far-UV circular dichroism (CD) (Caldinelli *et al.*, 2009).

The quantitative evaluation of solubility of protein samples was determined using a modified version of the method by (Mshayisa *et al.*, 2022). Each sample (10 mg) was dispersed in 1 ml of phosphate buffer (0.1 M K_2HPO_4 and KH_2PO_4 in a 1:1 molar ratio, adjusted to the required pH using 1 M HCl or 1 M KOH) and then incubated on a rotary shaker for 30 minutes at room temperature. The samples were centrifuged at 16 000×*g* for 20 minutes at 4 °C. The protein content of the supernatant was determined using the Bradford assay (Sigma-Aldrich, St Louis, MO, USA). Protein solubility was calculated as follows and expressed as a percentage:

$$\text{Solubility} = \frac{\text{protein content in supernatant}}{\text{total protein content in sample}} \times 100 \quad (1)$$

The amino acid and total protein content analysis was performed by Creative Proteomics (Shirley, NY, USA) by HPLC analysis. In detail, approx. 3 mg of each sample was soaked in 800 µl fresh performic acid overnight, then dried under a nitrogen flux. In parallel, basic hydrolysis was performed with 200 µl of 4.2 M NaOH at 110 °C for 24 hours; NaOH was then neutralised with 200 µl of 4.2 M HCl and 600 µl of norleucine dilution buffer was added. A third hydrolysis was performed with 200 µl of 6 M HCl-1% phenol at 110 °C for 24 hours: a sample of the supernatant (containing 2.0 nmol norleucine) was loaded for analysis into a Hitachi L-8900 Amino Acid Analyser.

Lipidomic analysis

The lipid extraction yields were determined as the weight ratio (%) to the initial dried insect biomass, after petroleum ether evaporation at 50 °C using a Laborota 4000 rotary evaporator (Heidolph, Schwabach, Germany). Lipid composition was analysed on 10 mg lipid extract, appropriately diluted, by mass spectrometry using an ExionLC™ AD system (SCIEX) connected to TripleTOF™ 6600 System (SCIEX) equipped with Turbo V™ Ion Source with ESI Probe at UNITECH OMICs (University of Milano, Italy) (Bruno *et al.*, 2025b; Furioso Ferreira *et al.*, 2025); two runs were performed for each extraction. For the lipidomic analysis, five independent biological replicates were used. To avoid the variance throughout the sample preparation, data acquisition and data pre-processing steps, quality control (QC) samples were analysed every 8 analyses. The QC samples were prepared to be qualitatively and quantitatively representative providing an average of all the lipids analysed.

Lipid analysis of polar species was performed by means of tandem mass spectrometry and mass spectral library search. Data processing was carried out using the untargeted data processing program MS-DIAL (v. 4.24; http://prime.psc.riken.jp/compms/msdial/main.html) with LipidBlast database v. 68 (https://fiehnlab.ucdavis.edu/projects/LipidBlast). Statistical analysis was performed using MetaboAnalyst software, version 5.0.

Peak intensities were $\log_2$ transformed, centred by subtracting the median within each replicate, and subjected to principal component analysis (PCA) by the Perseus software (Tyanova *et al.*, 2016) (Max-Planck-Institute of Biochemistry, Martinsried, Germany; version 1.5.8.5; http://www.perseus-framework.org). Log_2 data were then subjected to two-way ANOVA analysis to identify statistically significant differentially accumulated metabolites (DAMs) depending on the diet used to rear the larvae (regardless of the insect developmental stage), on the developmental stage of the insect (regardless of the diet), or by the interaction between these two factors. A false discovery rate (FDR) cut-off of 0.01 was considered to extrapolate statistically significant comparisons. We then generated a heatmap of the interaction-dependent DAMs using hierarchical clustering in Perseus with its default settings. Lipid Pathway Enrichment Analysis (LIPEA) software was used to perform the pathway enrichment analysis of metabolites (Acevedo *et al.*, 2018) using *Musca domestica* as background organism.

Proteomics and bioinformatic analysis

Proteomic analysis was performed using 2 g of whole larvae and pupae ground in liquid nitrogen. Four independent biological replicates were used. The powder obtained was then sonicated three times on ice in lysis buffer containing 7 M urea, 2 M thiourea and 1% protease inhibitor cocktail. After centrifugation at 12 000×*g* for 10 min at 4 °C, the supernatant was collected and the protein concentration determined. The extracted proteins were quantified using the Bradford assay (Bradford, 1976) and digested with trypsin via the filter aided sample preparation (FASP) technique (Wiśniewski, 2019). Tryptic peptides were analysed using a QExactive mass spectrometer, following established protocols (Domingo *et al.*, 2024). Raw data were processed with MaxQuant (v.1.5.3.3) to search against the *H. illucens* UniProt database. Search parameters included up to two missed cleavages, fixed carbamidomethylation of cysteine, and variable modifications of methionine (oxidation). Peptide length was set to a minimum of six amino acids, and precursor mass tolerance was 4.5 ppm for the primary search. Label-free quantification (LFQ) with match-between-runs (0.7 min window) and a target-decoy strategy (revert mode) was employed. Peptide and protein identifications were filtered to 1% false discovery rate (FDR), and known contaminants and non-consistent identifications were removed. Protein groups detected only in two of the four biological replicates were not considered for the analysis. Missing values were imputed using an in-house tool (Vannini *et al.*, 2019). MaxQuant output file hits were represented by a group of proteins (group of IDs) sharing the same set or a subset of peptides of the best matching leading protein. For bioinformatic analysis, only the leading protein was considered. Subsequent data processing such as $\log_2$ transformation, median centring of LFQ intensities, PCA and hierarchical clustering, were performed using Perseus software (http://www.perseus-framework.org). Hierarchical clustering was conducted with default settings. The mass spectrometry data have been deposited to the ProteomeXchange Consortium (http://proteomecentral.proteomexchange.org) via the jPOST partner repository (https://repository.jpostdb.org) with the data set identifier PXD068016 for ProteomeXchange and JPST004054 for jPOST (Okuda *et al.*, 2025).

Due to the limited annotation of the *H. illucens* proteome, a local BLAST search was performed against the *Drosophila melanogaster* protein database (downloaded from UniProt on May 1, 2025) to enable the use of specific bioinformatics tools. Only BLAST hits with an expectation value (e-value) score below 0.05 were considered. The enrichment analysis was performed using ShinyGO v0.82 (Ge *et al.*, 2022) with a *P*-value cutoff (FDR) of 0.05.

Lipid-related differentially abundant proteins (DAPs) were identified by examining protein GO terms and annotations across the following databases: InterPro (https://www.ebi.ac.uk/interpro/), Pfam (http://pfam.xfam.org/), KEGG (https://www.genome.jp/kegg/), UniProt (https://www.uniprot.org/), SMART (http://smart.embl-heidelberg.de/), STRING (https://string-db.org/), Reactome (https://reactome.org/), Monarch (https://monarchinitiative.org/), and WikiPathways (https://www.wikipathways.org/).

Correlation analysis between omics

The comprehensive, user-friendly platform OmicsAnalyst (https://www.omicsanalyst.ca/home.xhtml; Ewald *et al.*, 2024) was used for correlation analysis between lipidomic and proteomic data. Analysis parameters were as follows: Pearson correlation coefficient and threshold values between-omics of 0.5.

3 Results

Extraction and characterisation of protein, lipid and chitin components

The extraction of the different biological components from dried BSF larvae and pupae reared on both substrates was performed following the procedure reported in (Bruno *et al.*, 2025b). The amount of recovered lipids was higher in larvae especially when reared on the modified s-OFMSW, representing 42-44% of the starting material vs. 38-42% for pupae (Table 1). Proteins were recovered by precipitation at pH of minimum solubility (Smets *et al.*, 2020): a slightly higher amount of proteins was recovered from larvae and pupae reared on modified s-OFMSW (15.1 and 14.0%, respectively) in comparison with insects grown on s-OFMSW (12.9% at both developmental stages; Table 1).

Chitin was isolated by basic and acidic chemical treatments from the deproteinated residue. When s-OFMSW was used as rearing substrate, a higher chitin content (approx. 4.2%) was recovered from pupae compared to larvae, while using the modified s-OFMSW as rearing substrate, chitin was present to a larger extent in larvae (5.1%; Table 1). The soluble carbohydrate content was roughly the same among the samples, with an interesting rise in the total carbohydrate content in larvae

TABLE 1 Composition of the main components of BSF reared on two surrogate diets

	s-OFMSW (%)		Modified s-OFMSW (%)	
	Larvae	Pupae	Larvae	Pupae
Lipids	41.9 ± 1.2[a]	40.6 ± 1.1[a]	42.7 ± 1.0[a]	40.7 ± 0.4[a]
Protein	13.0 ± 0.5[a]	12.9 ± 0.7[a]	14.9 ± 1.6[a]	14.0 ± 9.7[a]
Defatted residue[1]	23.5 ± 1.0[a]	34.8 ± 0.7[b]	22.6 ± 0.5[a]	36.8 ± 0.8[b]
Chitin	3.0 ± 0.1[a]	4.2 ± 0.2[b]	2.9 ± 0.1[a]	4.7 ± 0.5[b]
Ash content	3.4 ± 0.1	2.7 ± 0.1	3.1 ± 0.1	3.6 ± 0.2
Soluble carbohydrates[2]	1.9 ± 0.1	1.7 ± 0.5	1.9 ± 0.2	1.8 ± 0.1
Total carbohydrates[3]	2.9 ± 0.1	3.2 ± 0.1	5.1 ± 0.2	2.7 ± 0.1

The results are expressed as the percentage of mass ratio with respect to the starting sample before defatting (approx. 20 g). Values represent the mean ± SEM of five replicates. Values sharing the same superscript lowercase letter (a, b) within a row are not significantly different from each other (one-way ANOVA, Tukey's HSD post hoc test, $P < 0.05$).

1 Dried solid pellet after removal of the soluble proteins, used for chitin extraction.

2 Carbohydrates determined as glucose equivalents on the resuspended protein extract; chitin and N-acetylglucosamine were not detected.

3 Carbohydrates determined as glucose equivalents on whole ground biomass after acid hydrolysis (3 M HCl, 3 h at 100 °C); chitin and N-acetylglucosamine were not detected.

TABLE 2 Protein extract composition from BSF reared on two different surrogate diets

	s-OFMSW (%)		Modified s-OFMSW (%)	
	Larvae	Pupae	Larvae	Pupae
Protein content[1]	93.6 ± 10.8	87.8 ± 7.8	79.6 ± 5.0	91.8 ± 3.9
Carbohydrate content[2]	5.5 ± 0.5	3.4 ± 0.2	1.5 ± 0.2	0.8 ± 0.1

The results are expressed as the mass ratio percentage with respect to the dried protein extract. Values represent the mean ± SEM of two replicates. In all cases, DNA level was below detection.

1 Determined using the ninhydrin method.

2 When the resuspended protein extract was centrifuged prior to measuring the carbohydrates recovery, no significant variation was observed.

compared to pupae when reared on modified s-OFMSW (5.1 vs 2.7%).

Altogether, the raw extraction yield of the three main biological components (i.e., lipids, proteins and chitin) was similar in samples from the two developmental stages, with a higher amount of deproteinated and defatted residue from pupae (Table 1).

Analysis of the protein fraction

The purity degree of the protein fraction, calculated by the ninhydrin assay, was between 80 and 92% for modified s-OFMSW and 88 and 94% for s-OFMSW. The amount of residual free carbohydrates in the protein extracts from the modified s-OFMSW varied between 0.8-1.5%, with a higher amount in larval extracts (Table 2). When the insoluble components were separated by centrifugation prior analysis, the carbohydrate content did not differ significantly (1.0 ± 0.1%).

Amino acid analysis showed that isolated protein fractions were rich in Asp/Asn, Glu/Gln, Leu, Ala, Gly, Lys, and Tyr in terms of molar ratios, and in Ala, Trp, Glu/Gln, Leu, Tyr, Lys, and Phe in terms of weight ratios (Table 3). Notably, larvae were enriched in Leu and Ala compared to pupae.

The solubility of the protein extracts from larvae reared on s-OFMSW and modified s-OFMSW is reported in Figure 1: in all cases, an increase was apparent at basic pH values. Notably, the proteins arising from the modified s-OFMSW possessed a higher solubility than the same fractions isolated from insects reared on the s-OFMSW at all pH values. Moreover, a significantly higher solubility was apparent for the proteins from pupae compared to larvae at pH values higher than 8-9.

In terms of secondary structure content of the protein fraction, the CD signal in the far-UV region between larvae and pupae reared on s-OFMSW was identical (Figure S1A in the Supplementary materials), while pupae reared on modified s-OFMSW showed a more intense negative peak in the 200 nm region compared to larvae (Figure S1B in the Supplementary materials).

TABLE 3 Amino acid analysis of the protein extracts from BSF reared on s-OFMSW and modified s-OFMSW

Amino acid	s-OFMSW				Modified s-OFMSW			
	Larvae (%)		Pupae (%)		Larvae (%)		Pupae (%)	
	Molar ratio	Weight ratio	Molar ratio	Weight ratio	Molar ratio	Weight ratio	Molar ratio	Weight ratio
Non-essential amino acids								
Asx[1]	11.14	11.43	12.60	12.66	11.72	11.92	12.51	12.64
Ser	4.94	3.84	4.60	3.50	4.73	3.64	4.66	3.56
Glx[2]	9.51	10.94	9.34	10.53	8.99	10.26	9.83	11.14
Pro	5.45	4.72	5.05	4.28	4.94	4.24	5.33	4.54
Gly	7.82	3.98	7.45	3.72	7.72	3.90	7.57	3.79
Ala	8.54	5.41	6.59	4.09	7.97	5.01	7.10	4.43
Tyr	5.55	8.08	6.46	9.20	6.15	8.87	6.16	8.83
Essential amino acids								
Thr	4.96	4.47	4.91	4.33	4.93	4.41	4.83	4.28
Arg	3.70	5.14	4.11	5.60	3.86	5.33	4.08	5.59
Cysteic acid	1.05	0.97	0.61	0.55	0.91	0.83	0.57	0.52
Val	6.26	5.53	6.10	5.28	6.31	5.53	5.99	5.21
Ile	5.14	5.19	4.98	4.92	5.16	5.17	4.89	4.86
Leu	8.31	8.38	7.80	7.71	8.35	9.36	7.80	7.75
Phe	4.94	6.48	5.40	6.94	5.19	6.75	5.09	6.58
His	2.55	3.12	2.83	3.39	2.68	3.25	2.82	3.39
Lys	6.65	7.59	7.26	8.13	6.82	7.73	7.04	7.92
Met sulfone	2.18	2.55	2.54	2.91	2.24	2.60	2.37	2.74
Trp	1.32	2.19	1.38	2.24	1.35	2.22	1.37	2.23

The results are expressed as percentage of the molar ratio and weight ratio for each amino acid.

1 Total Glu + Gln.

2 Total Asp + Asn.

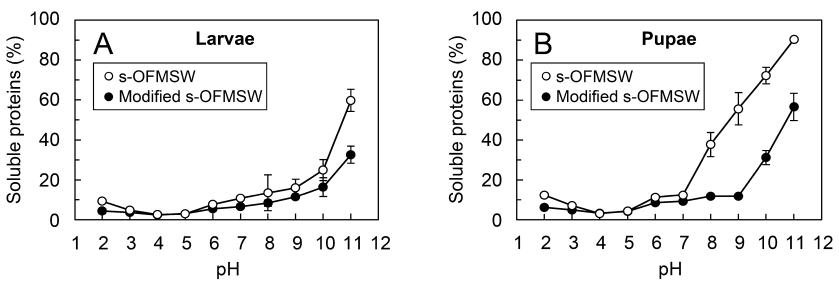

FIGURE 1 Solubility profile of proteins isolated from larvae (A) and pupae (B) reared on s-OFMSW (empty circle) (Bruno *et al.*, 2025b) and modified s-OFMSW (filled circle) at different pH values.

However, despite these spectral alterations, no significant difference in terms of secondary structure content, as predicted by DICHROWEB server, was evident between larvae and pupae (Miles *et al.*, 2022). On the contrary, comparing the protein fractions isolated at the same developmental stage, a higher content of α-helices and a lower content in β-strands was observed for samples reared on modified s-OFMSW than on s-OFMSW (s-OFMSW: larvae 15.0% helix, 31.1% strand, 20.9% turns; pupae: 17.6% helix, 28.9% strand, 21.9% turns; modified s-OFMSW: larvae: 20.0% helix, 18.7% strand, 26.2% turns; pupae: 23.0% helix, 14.0% strand, 25.4% turns).

Analysis of the lipid fraction

A total of 290 lipids, corresponding to 21 lipid subclasses, were identified and quantified in all samples (Table S3 in the Supplementary materials). Principal

component analysis (PCA) showed that biological replicates were plotted very closely in the PCA space, indicating a good correlation between replicates (Figure S2 in the Supplementary materials). The samples obtained from BSF pupae were separated in PC1 from those obtained from larvae and this accounted for approximately 68.2% of the total variation, indicating that the developmental stage strongly influenced the lipidome. The samples obtained from *H. illucens* reared on s-OFMSW were separated in PC2 from those obtained from insects fed with the modified s-OFMSW. This variation accounted for 23.7% of the total variation, suggesting a smaller effect of diet on lipid content than the developmental stage.

Identified lipids were then subjected to a two-way ANOVA test (FDR < 0.01) to determine statistically significant changes in the lipid composition due to the rearing substrate, the developmental stage of the insect, or an interaction between these two factors (Columns AC–AE in Table S3 in the Supplementary materials). Overall, s-OFMSW induced the accumulation of a greater number of lipids in *H. illucens*, regardless of developmental stage. In fact, 114 lipids increased in insects reared on s-OFMSW, while only 25 when the rearing substrate was the modified s-OFMSW (Table S4 in the Supplementary materials; Figure 2A). The s-OFMSW diet resulted mainly in the accumulation of triacylglycerols (TGs) and diacylglycerols (DGs) (Table S4 in the Supplementary materials; Figure 2A). Furthermore, fatty acids (FAs) and fatty acid esters of hydroxy fatty acids (FAHFAs) were present in large amounts and almost exclusively in BSF grown on s-OFMSW. On the other hand, the modified s-OFMSW only led to an accumulation of TGs, sphingomyelins (SMs) and few DGs, lysophosphatidylcholines (LPCs) and FAs. SMs accumulated only in larvae and pupae reared on modified s-OFMSW.

The insect's developmental stage affected lipid abundance, regardless of the diet used, with 98 lipids accumulated in BSF larvae and 63 in pupae (Table S5 in the Supplementary materials; Figure 2B). Larval lipids were characterised by many TGs, which were present mainly at this stage of development and represented 76.5% of differentially accumulated metabolites (Table S5 in the Supplementary materials; Figure 2B). Pupae, on the other hand, showed increased amounts of FAHFAs, and DGs and exclusively possessed monoglycerols (MGs), phosphatidylserines (PSs), phosphatidylethanolamines (PEs + lysophosphatidylethanolamine LPEs), and acylcarnitines (CARs).

Cluster analysis of 79 DAMs affected by an interaction of both factors (Figure 2C; Tables S6 and S7 in the Supplementary materials) revealed 4 main lipid profiles (clusters) in which lipids accumulated according to a specific combination of developmental stage and diet. Overall, the wider composition in lipids was found in larvae reared on s-OFMSW. Cluster 1 was mainly composed of FAHFAs found in larger amounts in larvae reared on s-OFMSW. In Cluster 2, among all conditions tested, TGs were mainly present in larvae reared on modified s-OFMSW, while PEs and PCs were more abundant in larvae and pupae reared on modified s-OFMSW diet and pupae reared on s-OFMSW (Cluster 3). FAs and some PSs (30:1, 34:1, 36:1) were more abundant in pupae reared on modified s-OFMSW and larvae reared on s-OFMSW (Cluster 4).

Pathway enrichment analysis of lipids revealed that glycerol phospholipid metabolism was the most enriched metabolic process in larvae and pupae fed with both diets (Table S8 in the Supplementary materials), while glycosylphosphatidylinositol (GPI) anchor biosynthesis and autophagy were processes enriched only in DAMs upregulated upon s-OFMSW. The metabolism of glycerophospholipids was enriched in both the larval and pupal developmental stages, regardless of the diet used. The metabolism of sphingolipids was enriched only in larvae, while GPI synthesis and autophagy were gene ontology (GO) terms enriched only considering the lipids accumulated in pupae. GPI-anchor biosynthesis, glycerophospholipid metabolism, and autophagy were the enriched processes in interaction-dependent DAMs.

Overview of proteomic profiles

To elucidate the molecular mechanisms driving the distinct responses of *H. illucens* larvae and pupae to s-OFMSW and modified s-OFMSW, quantitative proteomic analysis was conducted. This resulted in the identification and quantification of 1198 proteins (detailed in Table S9 in the Supplementary materials). Principal component analysis demonstrated high reproducibility among biological replicates (Figure S3 in the Supplementary materials). The PCA plot also revealed a clear separation of pupae and larvae samples along PC1, which explained 58.4% of the total variance, indicating a strong influence of developmental stage on the proteome. Furthermore, samples from insects reared on s-OFMSW and modified s-OFMSW separated along PC2, accounting for 14.9% of the variance, suggesting a less pronounced effect of diet compared to developmental stage, especially in larvae. The two-way ANOVA analysis

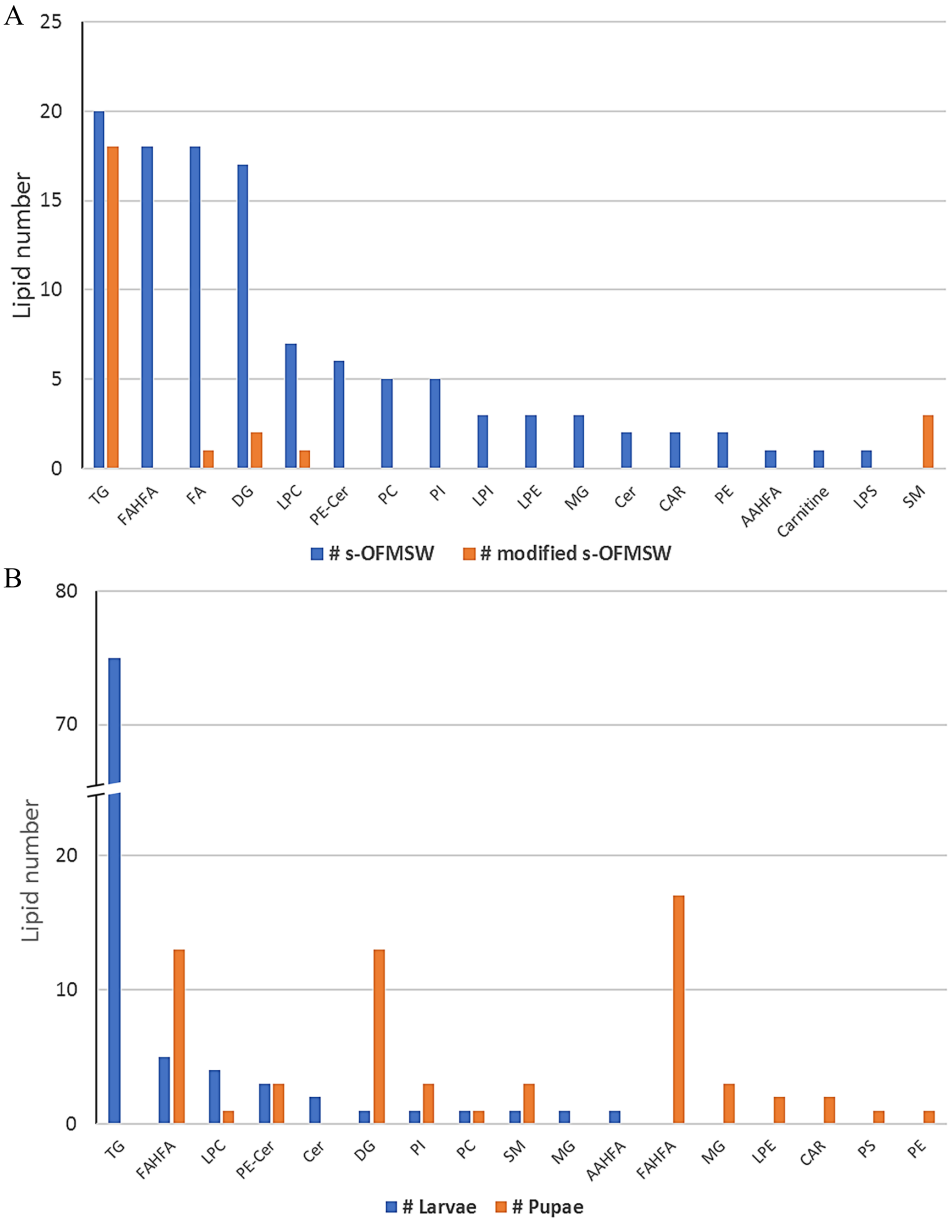

FIGURE 2 (A, B) Bar graph illustrating changes in lipid subclasses across (A) the two diets (s-OFMSW and modified s-OFMSW) and (B) the two insect developmental stages (larvae and pupae). (C) Heatmap and hierarchical clustering of the most discriminative lipid species among conditions. The relative abundance levels are depicted on the green-black-red scale. The four main clusters are shown. 1, BSF larvae reared on the s-OFMSW; 2, BSF pupae reared on the s-OFMSW; 3, BSF larvae reared on the modified s-OFMSW; 4, BSF pupae reared on the modified s-OFMSW. Abbreviations: AAHFA, acyl alpha-hydroxyl fatty acid; CAR, acylcarnitine, Cer, ceramide; DG, diacylglycerol; FA, fatty acid; FAHFA, fatty acyl esters of hydroxy fatty acid; LPC, lysophophatidylcholine, LPE, lysophosphatidylethanolamine; LPI, lysophosphatidylinositol; LPS, lysophosphatidylserine; MG, monoacylglycerol; PC, phosphatidylcholine; PE, phosphatidylethanolamine; PE-Cer, ceramide phosphoethanolamine; PI, phosphatidylinositol; PS, phosphatidylserine; SM, sphingomyelin; TG, triacylglycerol.

identified significant differences in protein abundance based on diet, developmental stage, and their interaction (FDR < 0.01). This analysis revealed that 83.6% of the identified proteins (1002 DAPs; Table S10 in the Supplementary materials) were differentially abundant. The single factors, diet and developmental stage, significantly influenced the abundance of 187 and 433 DAPs, respectively (Tables S11 and S12 in the Supplementary materials). Notably, 102 diet-dependent DAPs were more abundant in insects fed on modified s-OFMSW, irrespective of the developmental stage. Conversely, 147 and 286 proteins were more abundant in larvae and pupae, respectively. Finally, the interaction between diet and developmental stage significantly impacted the abundance of 501 proteins (Table S13 in the Supplementary materials).

C

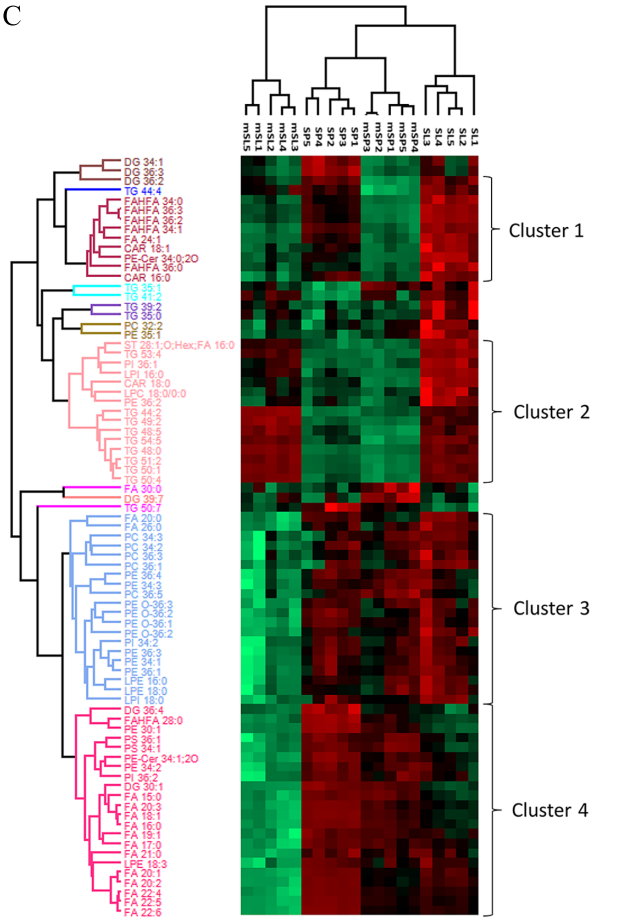

FIGURE 2 (Continued).

Cluster analysis of interaction-related DAPs identified 7 clusters, with 4 being the most prominent (Figure 3; Table S14 in the Supplementary materials), each characterised by a distinct protein profile. Specifically, clusters 1 and 2 contained proteins that were less and more abundant, respectively, in pupae reared on the s-OFMSW compared to other conditions. Clusters 4 and 5 comprised DAPs that were abundant only in larvae fed with the s-OFMSW and modified s-OFMSW, respectively.

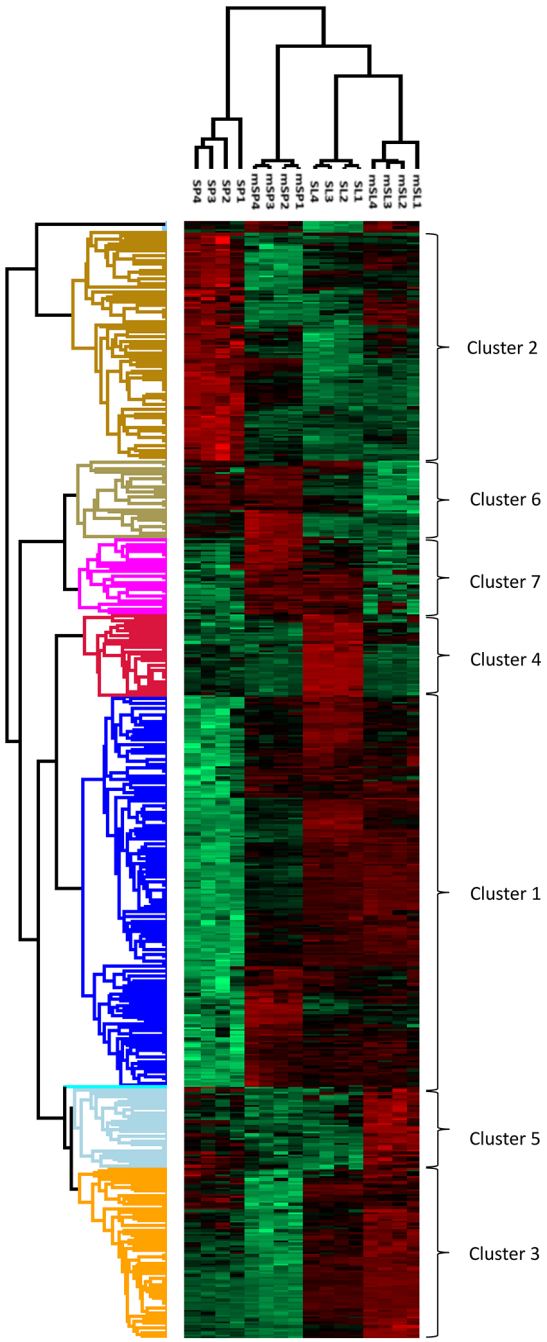

FIGURE 3 Heatmap and hierarchical clustering of differentially abundant proteins. The relative abundance levels are depicted on the green-black-red scale. The seven main clusters are shown. SL, BSF larvae reared on the s-OFMSW; SP, BSF pupae reared on the s-OFMSW; mSL, BSF larvae reared on the modified s-OFMSW; mSP, BSF pupae reared on the modified s-OFMSW.

Pathway enrichment analyses of DAPs

Enrichment analyses were performed to elucidate the biological function of DAPs. Since the *H. illucens* proteome has limited annotation and many proteins are uncharacterised, we used BLAST to search the *D. melanogaster* protein database for similar sequences. The results revealed specific biological processes enriched within both diet- and developmental stage-dependent DAPs. Proteins more abundant in insects fed on modified s-OFMSW were primarily associated with membrane assembly, acetyl-CoA synthesis, and the positive regulation of mRNA splicing (Figure 4A). Conversely, the most enriched processes among DAPs in larvae and pupae fed with s-OFMSW included fructose 1,6-bisphosphate metabolism, muscle contraction, and fatty acid oxidation (Figure 4B). The analysis also highlighted distinct biological processes enriched based on the insect's developmental stage, irrespective of the

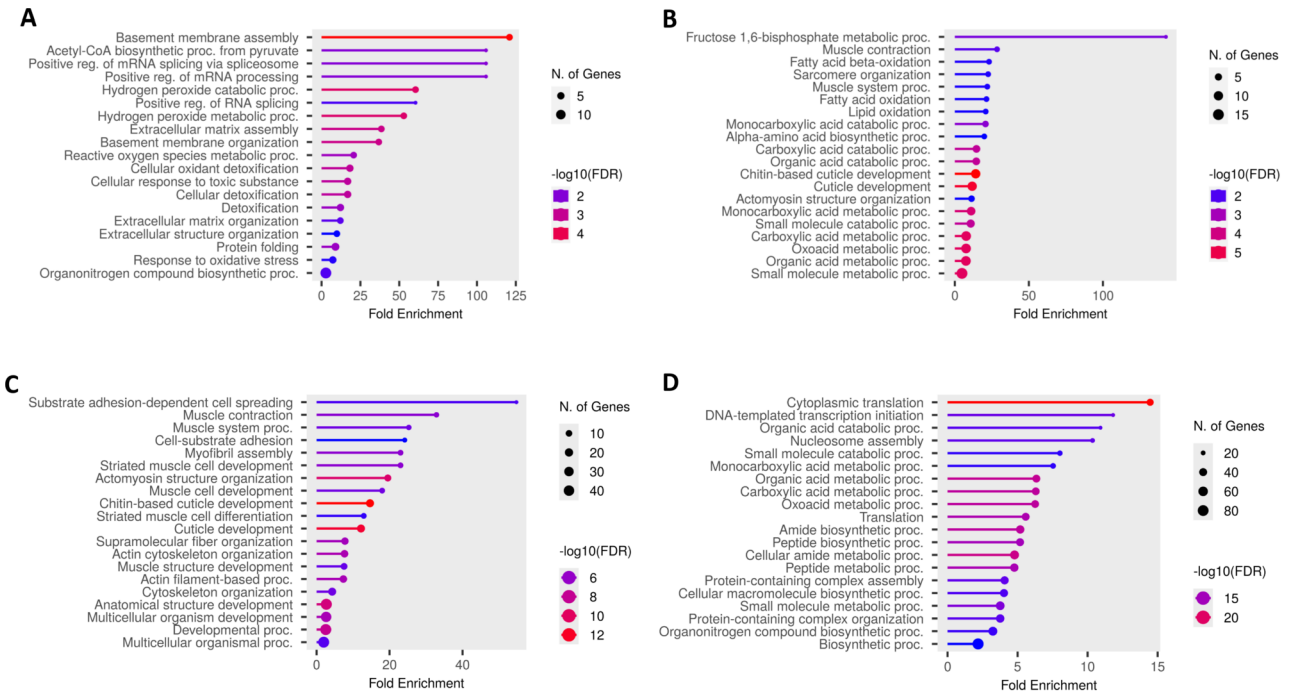

FIGURE 4 GO enrichment analysis of differentially abundant proteins accumulated in (A) BSF larvae and pupae reared on s-OFMSW; (B) BSF larvae and pupae reared on OFMSW; (C) larvae reared on both diets; (D) pupae reared on both diets.

diet. Specifically, muscle development and contraction, along with cuticle development, were enriched in larvae, while cytoplasmic translation, organic acid metabolic processes, nucleosome assembly, and peptide/amide synthesis were enriched in pupae (Figure 4C–D).

Among DAPs affected by an interaction of both factors, proteins of the selected cluster 1 were mainly involved in amino acid catabolic processes and fatty acid oxidation (Figure 5A). In proteins of cluster 2, the most enriched biological processes were glycolipid catabolic and proteasomal ubiquitin-independent protein catabolic processes (Figure 5B). β-alanine metabolism and fatty acid degradation were the most enriched GO terms among DAPs of cluster 4, while proteins in cluster 5 were mainly involved in hormone biosynthesis (Figure 5C–D).

A comprehensive functional annotation of the DAPs was conducted to pinpoint proteins involved in lipid metabolism and transport (Table S15–S17 in the Supplementary materials). This analysis revealed 32 lipid-related DAPs that were diet-dependent and 77 that were development-dependent. Specifically, 18 lipid-related DAPs showed increased abundance with the modified s-OFMSW, while 14 were more abundant with the s-OFMSW. Among the development-dependent lipid-related DAPs, a significant majority (68 DAPs, 89%) were more abundant in pupae compared to larvae (9 DAPs, 11%). Furthermore, the interaction between diet and developmental stage influenced the abundance of 89 lipid-related proteins, with the majority (45) belonging to cluster 1 (Figure S4 in the Supplementary materials).

Correlation analysis between lipidomics and proteomics

Correlation analysis was conducted to evaluate the strength and direction of relationships between different omics datasets and to understand the interconnectedness of biological organisation levels. A diagnostics plot illustrated the overall distribution of computed between-omics correlation values (Figure S5 in the Supplementary materials). The substantial number of values exceeding the set threshold (542 and 698) indicated statistically significant relationships between DAMs and DAPs. Specifically, 542 pairs of omics features showed a moderate to strong positive linear correlation, while 698 pairs exhibited a moderate to strong negative linear correlation.

4 Discussion

In this work we investigated the effect of two experimental substrates mimicking the OFMSW and having

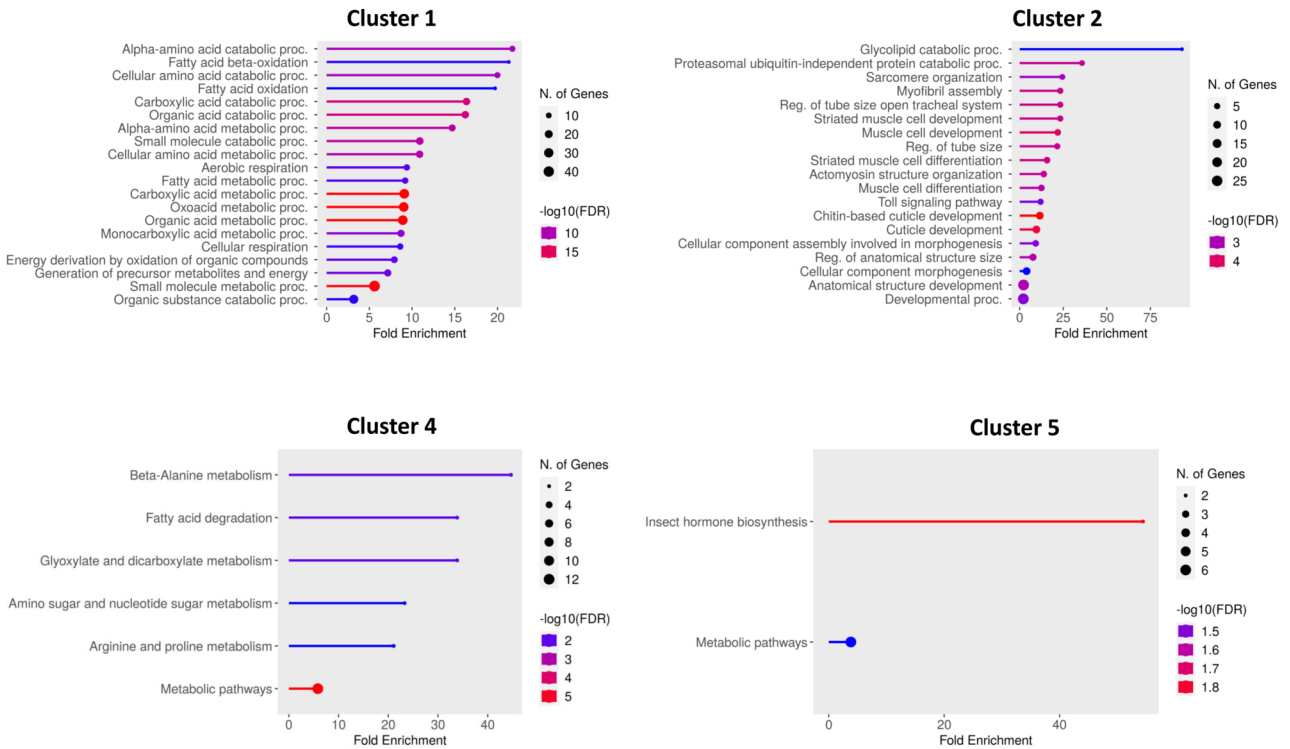

FIGURE 5 GO enrichment analysis of the differentially abundant proteins regulated by the interaction of diet and developmental stage and present in the four selected clusters (clusters 1, 2, 4 and 5).

different chemical composition and nutrient content on the main components of BSF larvae and pupae.

From a quantitative point of view, the lipidomic analysis revealed the greatest amount of lipids in larvae reared on s-OFMSW diet, in agreement with the highest level present in the diet. Larvae reared on surrogate substrates exhibited a higher protein content compared to BSF reared on r-OFMSW (Bruno *et al.*, 2025b), while pupae showed a lower content (Table 1). Interestingly, a reverse trend was observed for lipids (in particular, a very low amount is observed for pupae reared on r-OFMSW).

Notably, until now few works reported the carbohydrate content, in addition to protein and lipid level, in BSF reared on different food wastes (see Table 3 of Hopkins *et al.*, 2021) and the reported values show a significant degree of variability. Most consistent data were related to the profiles of larvae, with our data showing higher levels in essential amino acids (Table 3). The total percentage of essential amino acids is approx. 44% vs. 38% reported in Mshayisa *et al.* (2022). This enrichment is particularly relevant from a nutritional and industrial perspective, as essential amino acids determine protein quality and strongly influence the suitability of BSF biomass for feed and food applications. Higher levels of limiting amino acids such as lysine and methionine may reduce the need for dietary supplementation in animal feed formulations, thereby increasing the economic and functional value of BSF-derived proteins. The secondary structure content of the protein fractions isolated from BSF reared on s-diets compares well with those obtained with the r-OFMSW (Bruno *et al.*, 2025a). Indeed, a lower residual carbohydrate content is apparent in protein fractions isolated from insects reared on modified s-OFMSW (Table 2).

As H. illucens undergoes profound physiological transformations throughout its life cycle, its metabolic profile dynamically responds to both developmental cues and dietary factors. To capture a comprehensive picture of these coordinated metabolic changes and their regulatory networks, we performed a multi-omics strategy, involving lipidomic and proteomic investigations. Overall, PCA analysis revealed that the developmental stage had a stronger effect on the lipid and protein compositions of *H. illucens* compared to the diet. The statistically significant correlations between DAMs and DAPs, highlighted by between-omics correlation analysis, suggested the presence of shared regulatory pathways (Figure S5 in the Supplementary materials).

The pathway enrichment analysis of DAMs revealed that glycerophospholipid metabolism was the most enriched process among all conditions considered. Although this process is not among the most enriched considering DAPs, the functional analysis identified

some proteins involved in processes related to glycerolipid metabolism, such as the aldo-keto reductase 1B (M9PF61) and the aldehyde dehydrogenase domain-containing protein (A9UNE9), accumulated in larvae and pupae fed with modified s- and s-OFMSW diet, respectively. Moreover, in pupae, regardless of the diet, several DAPs were involved in glycerolipid metabolism (A1Z784, A9UNE9, M9PF61, P20007, Q4V403, Q7K569, Q9VHX4, Q9VN86, Q9VGE7, Q9Y125). Notably, a β-galactosidase (Q9VGE7) and a saposin-related protein (Q9Y125) were specifically linked to glycosphingolipid biosynthesis. This evidence may be related to metamorphosis, during which the insect experiences extensive tissue and organ remodelling: larval structures are largely removed through programmed cell death processes, while adult tissues differentiate from groups of undifferentiated cells. This process allows reshaping the body plan, leading to the development of adult-specific organs and functions (Tettamanti and Casartelli, 2019).

The predominance of triglycerides in larvae underscores the substantial energy reserves needed for the transition to the pupal stage. Indeed, TGs serve as the primary energy storage, fueling a large proportion of the energy-intensive transformation from larva to pupa, and subsequently to adult stage, through fatty acid oxidation. Some studies suggest that up to 95% of the energy for metamorphosis derives from this source (Wronska *et al.*, 2023). Moreover, muscle development and contraction were the most enriched processes revealed by proteomics, aligning with the larvae's need for movement, feeding, and growth. Cuticle development was also enriched, reflecting increasing in size and molting during the larval stage. Among DAPs involved in lipid metabolism and transport, the accumulation of the vitellogenin-like lipoprotein (Q9VF24) was evident. Vitellogenins are yolk precursor proteins, heavily loaded with lipids, including TGs, that are synthesised in the fat body (the insect's primary metabolic organ) and secreted into the haemolymph (Sappington and Raikhel, 1998).

The lipid profile shifted significantly in the pupae. The increase in FAHFAs and DGs at this developmental stage, along with the exclusive presence of MGs and CARs, suggests a dynamic lipid metabolism focused on energy mobilisation (CARs for fatty acid transport into mitochondria for oxidation, MGs as lipolysis products), membrane remodelling (PSs, PEs, LPEs are key membrane components), and potentially signalling (DGs, LPEs). The enriched processes in pupae – cytoplasmic translation, organic acid metabolic processes, nucleosome assembly, and peptide/amide synthesis – pointed towards the intense cellular reorganisation and synthesis of new body structures – required for metamorphosis. In fact, the cytoplasmic translation and the peptide/amide synthesis reflect the high demand for protein production. Nucleosome assembly is crucial for DNA replication and organisation during cell division and differentiation (Zhang *et al.*, 2020). Furthermore, the accumulation of proteins involved in organic acid metabolism likely supports energy production and biosynthesis.

Our results suggest that the two diets influenced *H. illucens* lipid and protein profiles in a distinct and coordinated manner. The s-OFMSW diet (richer in lipids) promoted the accumulation of energy-rich lipids (TGs, DGs, FAs, FAHFAs) and was associated with metabolic pathways like glycolysis and fatty acids turnover, as well as energy utilisation (muscle contraction). FAs (both derived from TGs and DGs) are the direct substrates for acyl-coenzyme A oxidase (B5RIN5), medium-chain specific acyl-CoA dehydrogenase (G3KKP7), and medium-chain acyl-CoA ligase ACSF2 (Q9VMR6), all proteins upregulated in BFS reared on s-OFMSW diet (Table S9). In particular, the acyl-CoA ligase ACSF2 activates FAs into acyl-CoAs, which are then metabolised by acyl-CoA oxidase (in peroxisomes for long-chain FAs) and medium-chain specific acyl-CoA dehydrogenase (in mitochondria for medium-chain FAs) through β-oxidation. Storage lipids like TGs and DGs, are broken down by lipases to release FAs, which then interact with these proteins. In addition to TGs and DGs, FAHFAs could also be metabolised to release FAs.

On the other hand, the modified s-OFMSW diet led to a higher accumulation of structural lipids (SMs, LPCs) and of energy storage compounds (TGs), which was linked to protein processes involved in membrane building, central metabolism (acetyl-CoA synthesis), and gene expression regulation. Some proteins accumulated in BSF reared on modified s-OFMSW diet could explain the huge TG accumulation observed with this diet. Among them, β-spectrin (M9PF16) levels showed a positive correlation with TG levels. Interestingly, some research in *D. melanogaster* suggests that spectrins might be involved in lipid uptake and lipid droplet organisation, potentially coupling lipid uptake at the plasma membrane to lipid droplet growth (Diaconeasa *et al.*, 2013). The lipid droplet subset dehydrogenase 1 (Q9W3K9) is directly associated with lipid droplet production, and plays a role in the metabolism of lipids stored within the droplet, potentially influencing their synthesis, breakdown, or modification (Liang and Liu, 2025). Moreover, the fatty acid binding protein

(Q9VGM2) accumulated in insects grown on modified s-OFMSW diet, facilitates the intracellular transport of fatty acids released from triglyceride breakdown (lipolysis) to mitochondria for β-oxidation or to other cellular compartments for various uses.

Finally, cluster analysis grouped proteins regulated by an interaction of diet and development based on their abundance patterns. Proteins of cluster 1, less abundant in pupae reared on the s-OFMSW diet compared to other conditions, were enriched in fatty acid oxidation pointing out that this process was less active in pupae reared on the s-OFMSW. The s-OFMSW diet induced a metabolic shift in the pupae, prioritising other energy-generating pathways over fatty acid oxidation. At the same time, the energy demand of pupae reared on s-OFMSW might be lower compared to other conditions, leading to a reduced need for both fatty acid oxidation and extensive triglyceride storage. Typically, reduced fatty acid oxidation would lead to a minor breakdown of fatty acid, increasing their levels in line with our lipidomic investigation highlighting a bigger amount of FAs (Table S4 in the Supplementary materials). The proteomic analysis identified significant differences in protein abundance based on diet, developmental stage, and their interaction (83.6% of the identified proteins were differentially abundant; Table S10 in the Supplementary materials). Such extensive proteomic variation, corroborated by PCA, underscores the profound physiological reorganisation inherent in metamorphosis, specifically the transition from larval nutrient sequestration to the structural remodelling and resource-saving mechanisms essential for pupal development (Pliantiangtam *et al.*, 2021).

Overall, these findings contribute to a deeper understanding of the metabolic plasticity of *H. illucens* and provide a solid basis for tailoring rearing strategies aimed at optimising the biochemical composition of insect biomass for specific biotechnological applications.

Supplementary materials

Data is available on https://doi.org/10.1163/23524588-bja10443 under Supplementary Materials.

Acknowledgements

Lipidomic analyses were carried out at OMICs, an advanced facility established by the University of Milano to support proteomic, lipidomic and metabolomic studies.

Author contributions

GD: Investigation (omics), methodology, data curation, formal analysis, visualisation, writing (review and editing). MM, MO, LB: Investigation (biochemistry), methodology, data curation, formal analysis. DB: Investigation (insects rearing), methodology, data curation, formal analysis, writing (review and editing). DC, FF, MF: Investigation (lipidomics), methodology, data curation, formal analysis, writing (review & editing). GT, GM, MC: Conceptualisation, funding acquisition, writing (original draft, review and editing). LP: Conceptualisation, supervision, writing (original draft, review and editing).

Conflict of interest

The authors declare no conflict or interest.

Data availability

The datasets generated for this study are available on request to the corresponding author. The mass spectrometry data have been deposited in the ProteomeXchange Consortium (identifier ID PXD068016).

Funding

This work was supported by Fondazione Cariplo (grant number 2020-0900) and the European Union Next – Generation EU (Piano Nazionale di Ripresa e Resilienza (PNRR) – missione 4 componente 2, investimento 1.4-D.D. 1032 17/06/2022, CN00000022).

References

Acevedo, A., Durán, C., Ciucci, S., Gerl, M. and Cannistraci, C.V., 2018. LIPEA: Lipid Pathway Enrichment Analysis. bioRxiv: 274969. https://doi.org/10.1101/274969

Bonomini, M.G., Prandi, B. and Caligiani, A., 2024. Black soldier fly (*Hermetia illucens L.*) whole and fractionated larvae: *In vitro* protein digestibility and effect of lipid and

chitin removal. Food Research International 196: 115102. https://doi.org/10.1016/j.foodres.2024.115102

Bradford, M.M., 1976. A rapid and sensitive method for the quantitation of microgram quantities of protein utilising the principle of protein-dye binding. Analytical Biochemistry 72: 248-254. https://doi.org/10.1016/0003-2697(76)90527-3

Bruno, D., Bonelli, M., Valoroso, M.C., Roma, D., Montali, A., Pellegrino, M.G., Marzari, M., Caccia, S., Tettamanti, G. and Casartelli, M., 2025a. Black soldier fly larvae efficiently bioconvert the organic fraction of municipal solid waste thanks to the functional plasticity of their midgut. Journal of Insects as Food and Feed 11: 157-172. https://doi.org/10.1163/23524588-00001193

Bruno, D., Orlando, M., Testa, E., Carnevale Miino, M., Pesaro, G., Miceli, M., Pollegioni, L., Barbera, V., Fasoli, E., Draghi, L., Baltrocchi, A.P.D., Ferronato, N., Seri, R., Maggi, E., Caccia, S., Casartelli, M., Molla, G., Galimberti, M.S., Torretta, V., Vezzulli, A. and Tettamanti, G., 2025b. Valorization of organic waste through black soldier fly: On the way of a real circular bioeconomy process. Waste Management 191: 123-134. https://doi.org/10.1016/j.wasman.2024.10.030

Bruno, D., Manas, F., Bonelli, M., Gold, M., Marzari, M., Roma, D., Valoroso, M.C., Montali, A., Guillaume, J.B., Rebora, M., Bressac, C., Herman, N., Caccia, S., Casartelli, M. and Tettamanti, G., 2025c. BugBook: Life cycle, reproduction, and morphofunctional characterisation of the gut, fat body, and haemocytes in the black soldier fly. Journal of Insects as Food and Feed 11: S289-S316. https://doi.org/10.1163/23524588-20250002

Bruno, D., Cuff, J.P., Adamaki-Sotiraki, C., Ameixa, O., Athanassiou, C.G., Boukrouh, S., Castellanos, F., Gebiola, M., Guillaume, J.B., Ibikunle, O., Klammsteiner, T., Oonincx, D., Savio, C., Sibinga, N.A., Tettamanti, G. and Opatovsky, I., 2026. Knowledge gaps in feeding physiology, microbiome and behaviour of insects for food and feed: overcoming barriers to advancing insect-rearing through interdisciplinarity, standardisation, and emerging technologies. Journal of Insects as Food and Feed 12: 1137-1147. https://doi.org/10.1163/23524588-20260004

Caldinelli, L., Molla, G., Sacchi, S., Pilone, M.S. and Pollegioni, L., 2009. Relevance of weak flavin binding in human D-amino acid oxidase. Protein Science 18: 801-810. https://doi.org/10.1002/pro.86

Caligiani, A., Marseglia, A., Leni, G., Baldassarre, S., Maistrello, L., Dossena, A. and Sforza, S., 2018. Composition of black soldier fly prepupae and systematic approaches for extraction and fractionation of proteins, lipids and chitin. Int. Food Res. 105: 812-820. https://doi.org/10.1016/j.foodres.2017.12.012

Chicea, D. and Nicolae-Maranciuc, A., 2024. A review of chitosan-based materials for biomedical, food, and water treatment applications. Materials 25: 5770. https://doi.org/10.3390/ma17235770

Diaconeasa, B., Harper Mazock, G., Mahowald, A.P. and Dubreuil, R.R., 2013. Genetic studies of spectrin in the larval fat body of *Drosophila melanogaster*: evidence for a novel lipid uptake apparatus. Genetics 195: 871-881. https://doi.org/10.1534/genetics.113.155192

Ewald, J., Zhou, G., Lu, Y., Kolic, J., Ellis, C., Johnson, J.D., Macdonald, P.E. and Xia, J., 2024. Web-based multi-omics integration using the Analyst software suite. Nature Protocols 19: 1467-1497. https://doi.org/10.1038/s41596-023-00950-4

Fisgativa, H., Tremier, A. and Dabert, P., 2016. Characterising the variability of food waste quality: a need for efficient valorisation through anaerobic digestion. Waste Manage. 50: 264-274. https://doi.org/10.1016/j.wasman.2016.01.041

Franco, A., Scieuzo, C., Salvia, R., Petrone, A.M., Taf, E., Moretta, A., Schmitt, E. and Falabella, P., 2021. Lipids from *Hermetia illucens*, an innovative and sustainable source. Sustainability 13: 10198. https://doi.org/10.3390/su131810198

Franco, A., Salvia, R., Scieuzo, C., Schmitt, E., Russo, A. and Falabella, P., 2022. Lipids from insects in cosmetics and for personal care products. Insects 13: 41. https://doi.org/10.3390/insects13010041

Furioso Ferreira, R., Ghaffari, M.H., Ceciliani, F., Fontana, M., Caruso, D., Audano, M., Savoini, G., Agazzi, A., Mrljak, V. and Sauerwein, H., 2025. Untargeted lipidomics reveals unique lipid signatures of extracellular vesicles from porcine colostrum and milk. PLoS ONE 20: e0313683. https://doi.org/10.1371/journal.pone.0313683

Ge, S.X., Jung, D. and Yao, R., 2022. ShinyGO: a graphical gene-set enrichment tool for animals and plants. Bioinformatics 15: 2628-2629. https://doi.org/10.1093/bioinformatics/btz931

Hahn, T., Tafi, E., von Seggern, N., Falabella, P., Salvia, R., Thomä, J., Febel, E., Fijalkowska, M., Schmitt, E., Stegbauer, L. and Zibek, S., 2022. Purification of chitin from pupal exuviae of the black soldier fly. Waste Biomass Valor. 13: 1993-2008. https://doi.org/10.1007/s12649-021-01645-1

Hopkins, I., Newman, L.P., Gill, H. and Danaher, J., 2021. The influence of food waste rearing substrates on black soldier fly larvae protein composition: a systematic review. Insects 12: 608. https://doi.org/10.3390/insects12070608

Kumar, S., Queiroz, L.S., Marie, R., Nascimento, L.G.L., Mohammadifar, M.A., de Carvalho, A.F., Brouzes, C.M.C., Fallquist, H., Fraihi, W. and Casanova, F., 2022. Gelling properties of black soldier fly (*Hermetia illucens*) larvae protein after ultrasound treatment. Food Chemistry 386: 132826. https://doi.org/10.1016/j.foodchem.2022.132826

Leni, G., Caligiani, A. and Sforza, S., 2019. Killing method affects the browning and the quality of the protein fraction of black soldier fly (*Hermetia illucens*) prepupae: a metabolomics and proteomic insight. Food Research International 115: 116-125. https://doi.org/10.1016/j.foodres.2018.08.021

Liang, B., Fu, L. and Liu, P., 2025. Regulation of lipid droplet dynamics and lipid homeostasis by hydroxysteroid dehydrogenase proteins. Trends in Cell Biology 35: 153-165. https://doi.org/10.1016/j.tcb.2024.10.010

Macwan, S., de Souza, T.S.P., Dunshea, F.R., DiGiacomo, K. and Suleria, H.A.R., 2024. Black soldier fly larvae (*Hermetica illucens*) as a sustainable source of nutritive and bioactive compounds, and their consumption challenges. Animal Production Science 64: AN23192. https://doi.org/10.1071/AN23192

Mersmann, L., Souza, V.G.L. and Fernando, A.L., 2025. Green processes for chitin and chitosan production from insects: current state, challenges, and opportunities. Polymers 17: 1185. https://doi.org/10.3390/polym17091185

Miceli, M., Pollegioni, L. and Molla, G., 2025. A pipeline for green and ultra-fast chitin extraction from black soldier fly larvae. Waste Biomass Valorization 16: 3085-3093. https://doi.org/10.1007/s12649-024-02843-3

Miles, A.J., Ramalli, S.G. and Wallace, B.A., 2022. DichroWeb, a website for calculating protein secondary structure from circular dichroism spectroscopic data. Protein Science 31: 37-46. https://doi.org/10.1002/pro.4153

Mohan, K., Sathishkumar, P., Rajan, D.K., Rajarajeswaran, J. and Ganesan, A.R., 2023. Black soldier fly (*Hermetia illucens*) larvae as potential feedstock for the biodiesel production: Recent advances and challenges. Science of The Total Environment 859: 160235. https://doi.org/10.1016/j.scitotenv.2022.160235

Mshayisa, V.V., Van Wyk, J. and Zozo, B., 2022. Nutritional, techno-functional and structural properties of black soldier fly (*Hermetia illucens*) larvae flours and protein concentrates. Foods 11: 724. https://doi.org/10.3390/foods11050724

Okuda, S., Yoshizawa, A.C., Kobayashi, D., Takahashi, Y., Watanabe, Y., Moriya, Y., Hatano, A., Takami, T., Matsumoto, M., Araki, N., Tabata, T., Iwasaki, M., Sugiyama, N., Kodera, Y., Tanaka, S., Goto, S., Kawano, S. and Ishihama, Y., 2025. jPOST environment accelerates the reuse and reanalysis of public proteome mass spectrometry data. Nucleic Acids Research 53: D462-D467. https://doi.org/10.1093/nar/gkae1032

Pimentel, A.C., Montali, A., Bruno, D. and Tettamanti, G., 2017. Metabolic adjustment of the larval fat body in Hermetia illucens to dietary conditions. Journal of Asia-Pacific Entomology 20: 1307-1313. https://doi.org/10.1016/j.aspen.2017.09.017

Pliantiangtam, N., Chundang, P. and Kovitvadhi, A., 2021. Growth performance, waste reduction efficiency and nutritional composition of black soldier fly (*Hermetia illucens*) larvae and prepupae reared on coconut endosperm and soybean curd residue with or without supplementation. Insects 12: 682. https://doi.org/10.3390/insects12080682

Praseatsook, K., Vachiraarunwong, A., Taya, S., Setthaya, P., Sato, K., Wanibuchi, H., Wongpoomchai, R., Dejkriengkraikul, P., Gi, M. and Yodkeree, S., 2025. Anticancer and antioxidant effects of bioactive peptides from black soldier fly larvae (*Hermetia illucens*). Nutrients 17: 645. https://doi.org/10.3390/nu17040645

Sadasivam, S. and Manickam, A., 2005. Biochemical methods. 2nd ed. New Age International, New Delhi.

Sappington, T.W. and Raikhel, A.S., 1998. Molecular characteristics of insect vitellogenins and vitellogenin receptors. Insect Biochemistry and Molecular Biology 28: 277-300. https://doi.org/10.1016/S0965-1748(97)00110-0

Siddiqui, S.A., van Greunen, L., Asma, Z., Bara, Y., Ali, A. and Mabelebele, M., 2024. The potential of chitin and chitosan from dead black soldier fly (BSF) (*Hermetia illucens*) for biodegradable packaging material – a critical review. Process Safety and Environmental Protection. 189: 1342-1367. https://doi.org/10.1016/j.psep.2024.06.108

Smets, R., Verbinnen, B., Van De Voorde, I., Aerts, G., Claes, J. and Van Der Borght, M., 2020. Sequential extraction and characterisation of lipids, proteins, and chitin from black soldier fly (*Hermetia illucens*) larvae, prepupae, and pupae. Waste Biomass Valorization 11: 6455-6466. https://doi.org/10.1007/s12649-019-00924-2

Starcher, B., 2001. A ninhydrin-based assay to quantitate the total protein content of tissue samples. Analytical Biochemistry 292: 125-129. https://doi.org/10.1006/abio.2001.5050

Testa, E., Fasoli, E., Riszo, P., Casartelli, M., Molla, G., Tettamanti, G. and Galimberti, M., 2025a. Amyloid-like self-assembling of black soldier fly proteins and development of bioplastics. ACS Sustainable Chemistry & Engineering 13: 18713-18726. https://doi.org/10.1021/acssuschemeng.5c07418

Testa, E., Barbera, V., Fasoli, E., Giese, U., Belviso, M.R., Rossini, P., Bruno, D., Tettamanti, G., Orlando, M., Molla, G., Casartelli, M. and Galimberti, M., 2025b. Electroconductive Bionanocomposites from black soldier fly proteins for green flexible electronics. ACS Sustainable Chemistry & Engineering 13: 2388-2400. https://doi.org/10.1021/acssuschemeng.4c08242

Tettamanti, G. and Bruno, D., 2024. Black soldier fly larvae should be considered beyond their use as feedstuff. Jour-

nal of Insects as Food and Feed 10: 1-7. https://doi.org/10.1163/23524588-241001ED

Tettamanti, G. and Casartelli, M., 2019. Cell death during complete metamorphosis. Philosophical Transactions of the Royal Society London Series B: Biological Sciences 374: 20190065. https://doi.org/10.1098/rstb.2019.0065

Tyanova, S., Temu, T., Sinitcyn, P., Carlson, A., Hein, M.Y., Geiger, T., Mann, M. and Cox, J., 2016. The Perseus computational platform for comprehensive analysis of (prote)omics data. Nature Methods 13: 731-740. https://doi.org/10.1038/nmeth.3901

Vannini, C., Marsoni, M., Scoccianti, V., Ceccarini, C., Domingo, G., Bracale, M. and Crinelli, R., 2019. Proteasome-mediated remodeling of the proteome and phosphoproteome during kiwifruit pollen germination. Journal of Proteomics 192: 334-345. https://doi.org/10.1016/j.jprot.2018.09.014

Wiśniewski, J.R., 2019. Filter aided sample preparation – a tutorial. Analytica Chimica Acta 1090: 23-30. https://doi.org/10.1016/j.aca.2019.08.032

Witono, J.R., Setyadi, F.F., Deandra, P.P., Wanta, K.C., Miryanti, A., Santoso, H., Astuti, D.A. and Bulin, C.D.Q.M., 2024. A comprehensive analysis of chitin extraction from the black soldier fly for chitosan production. Periodica Polytechnica Chemical Engineering 68: 507-522. https://doi.org/10.3311/PPch.23714

Wrońska, A.K., Kaczmarek, A., Boguś, M.I. and Kuna, A., 2023. Lipids as a key element of insect defense systems. Frontiers in Genetics 14: 1183659. https://doi.org/10.3389/fgene.2023.1183659

Zhang, W., Feng, J. and Li, Q., 2020. The replisome guides nucleosome assembly during DNA replication. Cell Bioscience 10: 37. https://doi.org/10.1186/s13578-020-00398-z